

The World Book Encyclopedia

© 2004 World Book, Inc. All rights reserved. This volume may not be reproduced in whole or in part in any form without prior written permission from the publisher.

World Book, Inc.
233 North Michigan Avenue
Chicago, IL 60601

www.worldbook.com

WORLD BOOK and the GLOBE DEVICE are registered trademarks or trademarks of World Book, Inc.

Copyright © 2003, 2002, 2001, 2000, 1999, 1998, 1997, 1996, 1995, 1994, 1993, 1992, 1991, 1990, 1989, 1988, 1987, 1986, 1985, 1984, 1983 by World Book, Inc.
Copyright © 1982, 1981, 1980, 1979, 1978 by World Book-Childcraft International, Inc.
Copyright © 1977, 1976, 1975, 1974, 1973, 1972, 1971, 1970, 1969, 1968, 1967, 1966, 1965, 1964, 1963, 1962, 1961, 1960, 1959, 1958, 1957 by Field Enterprises Educational Corporation.
Copyright © 1957, 1956, 1955, 1954, 1953, 1952, 1951, 1950, 1949, 1948 by Field Enterprises, Inc.
Copyright 1948, 1947, 1946, 1945, 1944, 1943, 1942, 1941, 1940, 1939, 1938 by The Quarrie Corporation.
Copyright 1937, 1936, 1935, 1934, 1933, 1931, 1930, 1929 by W. F. Quarrie & Company.
The World Book, Copyright 1928, 1927, 1926, 1925, 1923, 1922, 1921, 1919, 1918, 1917 by W. F. Quarrie & Company.
Copyrights renewed 1990, 1989, 1988, 1987, 1986, 1985, 1984, 1983 by World Book, Inc.
Copyrights renewed 1982, 1981, 1980, 1979, 1978 by World Book-Childcraft International, Inc.
Copyrights renewed 1977, 1976, 1975, 1974, 1973, 1972, 1971, 1970, 1969, 1968, 1967, 1966, 1965, 1964, 1963, 1962, 1961, 1960, 1958 by Field Enterprises Educational Corporation.
Copyrights renewed 1957, 1956, 1955, 1954, 1953, 1952, 1950 by Field Enterprises, Inc.

International Copyright © 2004, 2003, 2002, 2001, 2000, 1999, 1998, 1997, 1996, 1995, 1994, 1993, 1992, 1991, 1990, 1989, 1988, 1987, 1986, 1985, 1984, 1983 by World Book, Inc.
International Copyright © 1982, 1981, 1980, 1979, 1978 by World Book-Childcraft International, Inc.
International Copyright © 1977, 1976, 1975, 1974, 1973, 1972, 1971, 1970, 1969, 1968, 1967, 1966, 1965, 1964, 1963, 1962, 1961, 1960, 1959, 1958, 1957 by Field Enterprises Educational Corporation.
International Copyright © 1957, 1956, 1955, 1954, 1953, 1952, 1951, 1950, 1949, 1948 by Field Enterprises, Inc.
International Copyright 1948, 1947 The Quarrie Corporation.

Library of Congress Cataloging-in-Publication Data

The World Book encyclopedia.

p. cm.

Vol. 22 consists of research guide and index.

Summary: An encyclopedia designed especially to meet the needs of elementary, junior high, and senior high school students. Includes bibliographical references and index.

ISBN 0-7166-0104-4

1. Encyclopedias and dictionaries. II. Encyclopedias and dictionaries. I. World Book, Inc.

AE5 .W55 2004
031—dc21

2003010760

Printed in the United States of America

04 54321

H

H is the eighth letter in the alphabet used in Syria and Palestine. T and adapted an Egyptian for a twisted hank of ancient Greeks later to name it *eta*. They gave it its final capital form. of *h*. See Alphabet.

Uses. *H* or *h* ranks used letter in books, terial in English. In at and *Hindustan* in gec



Common forms of

Hh *Handwritten*

Handwritten letters vs from person to person. *script* (printed) letters, *h* have simple curves and straight lines. Cursive *le right*, have flowing lines

418 Human body

and grow. Most of the cells can also reproduce. A thin covering consisting of proteins and lipid molecules encloses each cell. This covering permits only certain substances to enter or leave the cell.

Nearly all the cells in the body are too tiny to see without a microscope. Yet packed within each cell is the machinery that the cell needs to carry out its many activities. For a detailed discussion of a cell's machinery and how it works, see the article *Cell* (Inside a living cell; The work of a cell).

The body has many basic kinds of cells, such as blood cells, muscle cells, and nerve cells. Each kind of cell has special features and jobs.

Cells of the same type form tissues. The body has four chief kinds of tissues. (1) *Connective tissue* helps support and join together various parts of the body. Most connective tissue is strong and elastic. (2) *Epithelial tissue* covers the body surface and so forms the skin. It also lines the mouth, the throat, and other passages and cavities inside the body. Epithelial tissue prevents harmful substances from entering the body. (3) *Muscle tissue* consists of threadlike fibers that can *contract* (shorten). Muscle tissue makes it possible for the body to move. (4) *Nervous tissue* carries signals. It permits various parts of the body to communicate with one another.

Organs and organ systems. An organ consists of two or more kinds of tissues joined into one structure that has a certain task. The heart, for example, is an organ whose job is to pump blood throughout the body. Connective tissue, epithelial tissue, muscle tissue, and nervous tissue make up the heart.

Groups of organs form organ systems. Each organ system carries out a major activity in the body. For example, the digestive system consists of various organs that enable the body to use food. Similarly, the nervous system is made up of organs that carry messages from one part of the body to another and processes them. The remainder of this article discusses the main organ systems of the human body. For more detailed descriptions of the major organs and organ systems, see the articles listed in the *Related articles* at the end of this article.

The skin

The skin is the largest organ of the body. The skin, including nails, hair, and sweat glands, is sometimes called the *integumentary system*. If the skin of a 150-pound (68-kilogram) person were spread out flat, it would cover approximately 20 square feet (1.9 square meters). Skin has two layers: the epidermis and the dermis. Subcutaneous tissues provide protection for the skin.

The epidermis forms the outermost layer of the skin. It serves as a barrier between the outside world and the inner tissues of the body. The outer portion of the epidermis consists of tough, dead cells that prevent bacteria, chemicals, and other harmful substances from entering the body. It also protects the body's inner tissues from the harsh rays of the sun and prevents the loss of water from these tissues.

The dermis is the lower layer of the skin. The dermis helps keep the temperature of the body within its normal range. The body produces tremendous amounts of heat as it uses food. Some of this heat escapes from the body through the blood vessels in the dermis. When the

body needs to retain heat, these blood vessels narrow and so limit heat loss. When the body needs to give off heat, the blood vessels in the dermis expand and so increase heat loss. The sweat glands, which come from the epidermis, also help control body temperature. These glands produce sweat, which is released through pores on the skin surface. As the sweat evaporates from the surface, it cools the body.

The dermis also serves as an important sense organ. Nerve endings within the dermis respond to cold, heat, pain, pressure, and touch.

Subcutaneous tissues lie directly beneath the skin. They provide extra fuel for the body. The fuel is stored in fat cells. Subcutaneous tissues also help retain body heat and cushion the inner tissues against blows to the body.

The skeletal system

The skeleton of an adult consists of more than 200 bones. The skeleton forms a strong framework that supports the body. It also helps protect the internal organs. For example, the brain is shielded by the skull, the spinal cord by the spinal column, and the heart and lungs by the ribs.

The skeleton works together with the muscles in enabling the body to move. The bones of the shoulders and arms, for instance, serve as levers against which the muscles that move the arm can pull. The place where bones meet is called a joint. There are two basic kinds of joints. (1) *Movable joints*, such as the elbow, knee, and shoulder joints, permit varying degrees of motion. The bones of a movable joint are held together by bundles of tough, flexible connective tissue called *ligaments*. (2) *Immovable joints* do not permit any movement of the bones. The bones of the skull, except for the jawbones, meet in immovable joints.

The skeleton serves as more than a framework for the body and a system of levers to help move the body. Bone tissue contains various kinds of cells that play a major role in maintaining the health of the blood. The cells of red bone *marrow*—the soft, fatty core of many bones—produce new blood cells and release them into the bloodstream. Yellow bone marrow, the most common type of marrow in the adult skeleton, stores fat. Yellow bone marrow does not normally produce blood cells.

Two kinds of bone cells regulate the mineral content of the blood. One kind removes calcium, phosphorus, and other minerals from the blood and deposits them in the bone. The other kind dissolves old mineral deposits and releases the minerals back into the bloodstream as needed.

The muscular system

The muscular system moves the body. The body has almost 700 muscles, each of which consists of special fibers that can contract. When a muscle contracts, it pulls the tissue to which it is attached. This pulling results in movement.

The muscles of the human body can be divided into two main types: (1) skeletal muscles and (2) smooth muscles. A third kind of muscle, *cardiac muscle*, is found only in the heart. It has features of both skeletal muscle and smooth muscle.

Skeletal muscles are the muscles that move the bones of the skeleton. They are attached to the skeleton by tendons. They are made up of skeletal muscles, and so *muscles*. The fibers that make up skeletal muscles alternate light and dark bands.

One end of each skeletal muscle is attached to a bone that does not move when the body moves. The other end of the muscle is attached to a bone, either directly or through a piece of connective tissue called a tendon. The muscle moves when the muscle contracts.

Muscles move the bones of the body. Muscles therefore contract and relax to move the body, such as the raising and lowering of the arm. One set pulls the bones in one direction. Another set pulls the bones in the opposite direction. For example, one set of muscles pulls the forearm down, and another set pushes the forearm up. The second set of muscles moves the forearm in the opposite direction.

Smooth muscles are found in internal organs. Unlike skeletal muscles, smooth muscles do not have striations. Smooth muscles move the stomach and intestines, the urinary system, and the digestive system. Smooth muscles also line the walls of the blood vessels and the passages. In all these cases, smooth muscles contract and relax automatically. We do not consciously control them. For example, the heart is called *involuntary muscle*. Smooth muscles cannot be seen with the naked eye. But smooth muscles are everywhere.

Ligaments and tendons





Medical Dictionary

222 entries found for artery.
To select an entry, click on it. (Click 'Go' if nothing happens.)

Go

artery

alveolar artery

angular artery

anterior cerebral artery

anterior choroid artery

anterior communicating artery

Main Entry: artery
Pronunciation: 'ärt-&-rē
Function: *noun*
Inflected Form(s): *plural -ter-ies*
: any of the tubular branching muscular- and elastic-walled vessels that carry blood from the heart through the body
[artery illustration]

Search here for another word:

SEARCH

Look it up

Merriam-Webster

Pronunciation Key

l&\ as a and u in about	lch\ as ch in chin	lo\ as aw in law
l&\ as e in kitten	le\ as in bet	lo\ as y in boy
l&r\ as ur and er in further	lE\ as ea in easy	lth\ as th in thin
la\ as a in ash	lg\ as g in go	lth\ as th in the
la\ as a in ace	li\ as i in hit	lu\ as oo in loot
la\ as o in mop	li\ as i in ice	lu\ as oo in foot
lau\ as ou in out	lj\ as j in job	ly\ as y in yet
	l(ng)\ as ng in sing	lzh\ as si in vision
	lo\ as o in go	

© 2003 by Merriam-Webster, Incorporated

The New Encyclopædia Britannica

Volume 16

MACROPÆDIA

Knowledge in Depth

FOUNDED 1768
15TH EDITION



Encyclopædia Britannica, Inc.
Jacob E. Safra, Chairman of the Board
Ilan Yeshua, Chief Executive Officer

Chicago
London/New Delhi/Paris/Seoul
Sydney/Taipei/Tokyo

First Edition 1768-1771
 Second Edition 1777-1784
 Third Edition 1788-1797
 Supplement 1801
 Fourth Edition 1801-1809
 Fifth Edition 1815
 Sixth Edition 1820-1823
 Supplement 1815-1824
 Seventh Edition 1830-1842
 Eighth Edition 1852-1860
 Ninth Edition 1875-1889
 Tenth Edition 1902-1903

Eleventh Edition
 © 1911
 By Encyclopædia Britannica, Inc.

Twelfth Edition
 © 1922
 By Encyclopædia Britannica, Inc.

Thirteenth Edition
 © 1926
 By Encyclopædia Britannica, Inc.

Fourteenth Edition
 © 1929, 1930, 1932, 1933, 1936, 1937, 1938, 1939, 1940, 1941, 1942, 1943,
 1944, 1945, 1946, 1947, 1948, 1949, 1950, 1951, 1952, 1953, 1954,
 1955, 1956, 1957, 1958, 1959, 1960, 1961, 1962, 1963, 1964,
 1965, 1966, 1967, 1968, 1969, 1970, 1971, 1972, 1973
 By Encyclopædia Britannica, Inc.

Fifteenth Edition
 © 1974, 1975, 1976, 1977, 1978, 1979, 1980, 1981, 1982, 1983, 1984, 1985,
 1986, 1987, 1988, 1989, 1990, 1991, 1992, 1993, 1994, 1995, 1997, 1998, 2002
 By Encyclopædia Britannica, Inc.

© 2002
 By Encyclopædia Britannica, Inc.

Copyright under International Copyright Union
 All rights reserved under Pan American, Berne
 and Universal Copyright Conventions by
 Encyclopædia Britannica, Inc.

No part of this work may be reproduced or utilized
 in any form or by any means, electronic or mechanical,
 including photocopying, recording, or by any
 information storage and retrieval system, without
 permission in writing from the publisher.

Printed in U.S.A.

Library of Congress Control Number: 2001089897
 International Standard Book Number: 0-85229-787-4

Britannica may be accessed at <http://www.britannica.com> on the Internet.

20020915
 125229 787-4

of blood pressure. Decreased blood flow to the kidney, changes in posture, or blockage of one or both renal (kidney) arteries may lead to increased production of the enzyme renin by the kidney. This substance causes development in the circulating blood of the substance angiotensin II, which causes blood vessels to contract, with resultant increase in blood pressure.

Receptors in great veins, in the aortic arch (the bend in the aorta above the heart), and the carotid sinus are sensitive to changes in blood pressure as blood is forced from the ventricles. These receptors, known as baroreceptors, help to modify shifts in pressure. When the receptors are stimulated by a rise in arterial pressure, which distends the arterial wall, reflexes are initiated that have an inhibiting effect on the heart, causing it to beat more slowly and with less force. At the same time there is a decrease in the constriction of the blood vessels. A fall in pressure, on the other hand, causes increased sympathetic and decreased parasympathetic nervous stimulation, with resultant increased heart rate and also a subsequent constriction of the blood vessels.

The force of the heartbeat depends on the initial length of the heart muscle fibres, the length of the pause in diastole, the oxygen supply, and the integrity and mass of the heart muscle, or myocardium. The greater the initial length of the muscle fibres in the heart, the more forceful will be the contraction. Artificially increasing venous return of blood to the heart distends the heart and intensifies the force of the beat. The greater inflow is handled by an increased output of the heart, without a change in its rate. When the ventricle does not completely fill (for example, after loss of blood), the force of the heartbeat is reduced. When the venous inflow during diastole is increased, as in muscular exercise, the beats become more forceful. If, as a result of excessive filling, the fibres are overstretched, a weak contraction results, with diminished cardiac output; consequently, the heart does not adequately empty itself. The force of the heart is also diminished if the diastolic phase is too short and there is inadequate filling.

Blood pressure is measured with a device called a sphygmomanometer. The pressure of blood within the artery is balanced by an external pressure exerted by air contained in a cuff applied externally around the arm. Actually, it is the pressure within the cuff that is measured. The steps employed in determining blood pressure with a sphygmomanometer are:

1. The cuff is wrapped securely around the arm above the elbow.
2. Air is pumped into the cuff with a rubber bulb until pressure is sufficient to stop the flow of blood in the brachial artery (the principal artery of the upper arm). Pressure within the cuff is shown on the scale of the sphygmomanometer.
3. The observer places a stethoscope over the brachial artery just below the elbow and gradually releases the air from within the cuff. The decreased air pressure permits the blood to flow, filling the artery below the cuff. Faint tapping sounds corresponding to the heartbeat are heard. When the sound is first noted, the air pressure within the cuff is recorded on the scale. This pressure is equal to the systolic blood pressure.
4. As the air in the cuff is further released, the sounds become progressively louder, until the sounds change in quality from loud to soft and finally disappear. The point at which the sound completely disappears should be recorded as diastolic blood pressure.

THE BLOOD VESSELS

Because of the need for the early development of a transport system within the embryo, the organs of the vascular system are among the first to appear and to assume their functional role. In fact, this system is established in its basic form by the fourth week of embryonic life. At approximately the 18th day of gestation, cells begin to group together between the outer skin (ectoderm) and the inner skin (endoderm) of the embryo. These cells soon become rearranged so that the more peripheral ones join to form a continuous flattened sheet enclosing more centrally placed cells; these cells remain suspended in a fluid medium as

primitive blood cells. The tubes then expand and unite to form a network; the primitive blood vessels thus appear.

The blood vessels consist of a closed system of tubes that transport blood to all parts of the body and back to the heart. As in any biologic system, structure and function of the vessels are so closely related that one cannot be discussed without the other's being taken into account.

Arteries transport blood to body tissues under high pressure, which is exerted by the pumping action of the heart. The heart forces blood into these elastic tubes, which recoil, sending blood on in pulsating waves. It is, therefore, imperative that the vessels possess strong, elastic walls to ensure fast, efficient blood flow to the tissues.

The wall of an artery consists of three layers (Figures 15 and 16), the innermost consisting of an inner surface of smooth endothelium covered by a surface of elastic tissues: the two form the tunica intima. The tunica media, or middle coat, is thicker in arteries, particularly in the large arteries, and consists of smooth muscle cells intermingled with elastic fibres. The muscle-cell and elastic fibres circle the vessel. In larger vessels the tunica media is composed primarily of elastic fibres. As arteries become smaller, the number of elastic fibres decreases while the number of smooth muscle fibres increases. The outer layer, the tunica adventitia, is the strongest of the three layers. It is composed of collagenous and elastic fibres. (Collagen is a connective-tissue protein.) The tunica adventitia provides a limiting barrier, protecting the vessel from overexpansion. Also characteristic of this layer is the presence of

Three layers of the artery wall

From S. Jacob and C. Franccone, *Structure and Function in Man* (1970); W.B. Saunders Co.

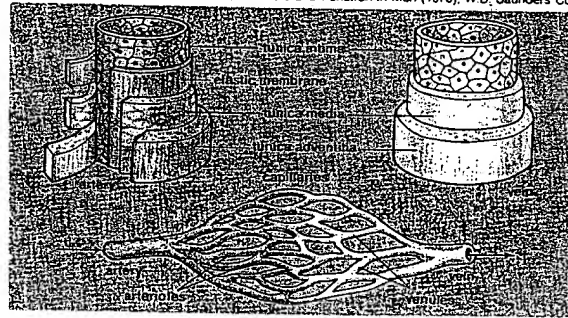


Figure 15: Component parts of arteries and veins.

small blood vessels called the vasa vasorum that supply the walls of larger arteries and veins; the inner and middle layers are nourished by diffusion from the blood as it is transported. The thicker, more elastic wall of arteries enables them to expand with the pulse and to regain their original size.

The transition from artery to arteriole is a gradual one, marked by a progressive thinning of the vessel wall and a decrease in the size of the lumen, or passageway. The tunica intima is still present as a lining covered by a layer of thin longitudinal fibres. A single layer of circular or spiral smooth muscle fibres now makes up the tunica media, and the tunica adventitia consists of connective tissue elements.

Being the last small branches of the arterial system, arterioles must act as control valves through which blood is released into the capillaries. The strong muscular wall of arterioles is capable of completely closing the passageway or permitting it to expand to several times its normal size, thereby vastly altering blood flow to the capillaries. Blood flow is by this device directed to tissues that require it most.

As the arterioles become smaller in size, the three coats become less and less definite, the smallest arterioles consisting of little more than endothelium, or lining, surrounded by a layer of smooth muscle. The microscopic capillary tubules consist of a single layer of endothelium, a continuation of the innermost lining cells of arteries and veins.

As the capillaries converge, small venules are formed whose function it is to collect blood from the capillary beds (i.e., the networks of capillaries). The venules consist of an endothelial tube supported by a small amount of collagenous tissue and, in the larger venules, by a few smooth muscle fibres as well. As venules continue to increase in

force of cardiac contraction

Diastole and systole

Blackwell Synergy

Home Browse Search My Synergy Register Help

dr james elia

Username Password

Sign In Login


You are at: [Home](#) > [List of Issues](#) > [Table of Contents](#) > Full Text

ANNOUNCING A NEW GORDON RESEARCH CONFERENCE
CRANIOFACIAL MORPHOGENESIS & TISSUE REGENERATION
 JANUARY 10-23 2004 VENTURA BEACH/HARRITT VENTURA, CA
 CHECK WWW.GRC.ORG FOR DETAILS

List of Issues
 Table of Contents
 < Prev Article Next Article >

Add to Favorite Articles
 E-mail this to a Friend

Full Article

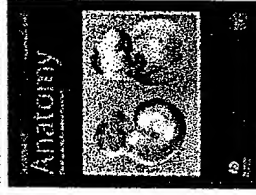
 [View/Print PDF article \(312K\)](#)

Download to reference manager

Journal of Anatomy

Volume 203 Issue 1 Page 89 - July 2003

doi:10.1046/j.1469-7580.2003.00195.x



Muscle satellite (stem) cell activation during local tissue injury and repair

Maria Hill,¹ A. Wernig² and G. Goldspink¹

Abstract

In post-mitotic tissues, damaged cells are not replaced by new cells and hence effective local tissue repair mechanisms are required. In skeletal muscle, which is a syncytium, additional nuclei are obtained from muscle satellite (stem) cells that multiply and then fuse with the damaged fibres. Although insulin-like growth factor-1 (IGF-1) had been previously implicated, it is now clear that muscle expresses at least two splice variants of the IGF-1 gene: a mechanosensitive, autocrine, growth factor (MGF) and one that is similar to the liver type (IGF-1Ea). To investigate this activation mechanism, local damage was induced by stretch combined with electrical stimulation or injection of bupivacaine in the rat anterior tibialis muscle and the time course of regeneration followed morphologically. Satellite cell activation was studied by the distribution and levels of expression of M-cadherin (M-cad) and related to the expression of the two forms of IGF-1. It was found that the following local damage MGF expression preceded that of M-cad whereas IGF-1Ea peaked later than M-cad. The evidence suggests therefore that an initial

QuickSearch in:

- ☒ Synergy
☐ PubMed (MEDLINE)

for

Authors:

- ☐ Maria Hill
☐ A. Wernig
☐ G. Goldspink

Key words

- ☐ IGF-1
☐ MGF

Related Articles

pulse of MGF expression following damage is what activates the satellite cells and that this is followed by the later expression of IGF-1Ea to maintain protein synthesis to complete the repair.

Introduction

Go to:

- ☐ M-cadherin
☐ muscle
☐ satellite cells

Satellite cells in skeletal muscle were first described by Mauro (1961) and it is now realized that these cells provide the extra nuclei for post-natal growth (Moss & Leblond, 1970; Schultz, 1996) and that they are also involved in repair and regeneration following local injury of muscle fibres (Grounds, 1998). In normal adult undamaged tissue the satellite cells are quiescent and usually detected just beneath the basal lamina. They express M-cadherin (M-cad) (Bornemann & Schmalbruch, 1994; Irintchev et al. 1994) and co-express myogenic factors including c-met, MyoD and myf5 and later myogenin (Cornelison & Wold, 1997; Beauchamp et al. 2000; Qu-Petersen et al. 2002). The origins of satellite cells are still somewhat uncertain as they were thought to be residual myoblasts (reviewed by Seale & Rudnicki, 2000) but there is accumulating evidence that they may also originate from pluripotent stem cells derived from progenitor cells of the vasculature (De Angelis et al. 1999). Pluripotent stem cells from bone marrow cells (Ferrari et al. 1998), as well as epidermal cells (Pye & Watt, 2001), have also been shown to fuse and adopt the muscle phenotype when introduced into dystrophic muscle.

It has been established that even in normal muscle, local injury does occur from time to time (Wernig et al. 1990) but in certain diseases such as the muscular dystrophies, the muscle fibres are markedly more susceptible to damage, in particular to the membrane (Cohn & Campbell, 2000). The contractile system of muscle fibres also sustains damage during eccentric contractions, i.e. when the muscle is activated while being stretched. It is interesting to note that the forces generated by activation combined with stretch exceed even those of maximal isometric contraction. In the muscle fibres involved, the sarcomeres may be pulled out to such a degree that there is no longer any overlap of the actin and myosin filaments, thus causing damage (Lieber & Friden, 1999).

During embryonic differentiation, mononucleated myoblasts first proliferate and then fuse to form myotubes that become innervated and develop into muscle fibres. Following fusion, no further mitotic divisions occur within the myotubes or muscle fibres. The extra nuclei required for growth are provided by satellite cells fusing with muscle fibres principally at their termini (Aziz-Ullah & Goldspink, 1974), which is the region responsible for longitudinal growth (Griffin et al. 1971; Williams & Goldspink, 1971, 1976; Tabary et al. 1972). When muscle fibres sustain damage they have to obtain extra nuclei for the repair process reasonably quickly, to avoid cell death, which would result in a decrease in muscle mass and a permanent functional deficit. The extra set of genes required for protein synthesis during repair is derived from satellite cells typically located between the basal lamina and the sarcolemma. However, it has not been apparent which factors are involved in activating these cells to multiply and fuse with damaged or growing muscle fibres. As insulin-like growth factor-I (IGF-I) has been implicated (see review by Adams, 1998), it seemed

Accepted for publication 2 May 2003

Affiliations

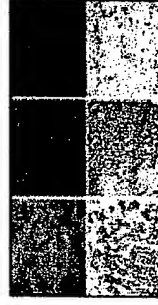
¹Basic Medical Sciences and Department of Surgery, Royal Free and University College Medical School, London University, UK

²Department of Physiology, University of Bonn, Germany

Correspondence

Correspondence
 Professor Geoffrey Goldspink,
 Basic Medical Sciences, Royal Free and University College Medical School, Rowland Hill Street, London NW3 2PF, UK.
 Tel.: +44 (0)20 78302410; e-mail: goldspink@rfc.ucl.ac.uk

Image Previews



[Full Size]

Fig. 1 Transverse sections of rat TA muscle stained with haematoxylin and eosin demonstrating maximal ...

relevant to measure expression levels of two insulin-like splice variants following imposed local damage. These were the systemic IGF-IEa and an autocrine splice variant produced by muscle (MGF). The latter was recently cloned from stretched/stimulated muscle (Yang et al. 1996) and, for this reason, and the fact that it has a different sequence to systemic IGF-I, it has been called mechano growth factor (MGF). IGF-I is reportedly involved in satellite cell activation (reviewed by Chakravarthy et al. 2001), although these *in vitro* studies may not accurately reflect what is happening *in vivo*, particularly in mature muscle when subjected to damage. Recent *in vivo* studies have indicated that MGF has different expression kinetics to IGF-IEa (Haddad & Adams, 2002) and this and other studies (Owino et al. 2001; Yang & Goldspink, 2002) suggest they have different modes of action.

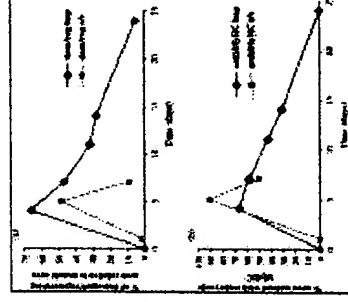
Repair following skeletal muscle damage has been observed in experimental models and certain features are common. Fibre degeneration with subsequent influx of leucocytes into the damaged area predominates in the first few days. Regeneration begins once the phagocytic inflammatory cells clear necrotic tissue. This phase of muscle remodelling is characterized by activation of undifferentiated skeletal muscle precursor cells or satellite cells. Cell adhesion molecules, for example M-cad and N-CAM, have previously (Irintchev et al. 1994; Qu-Petersen et al. 2002) been shown to be expressed in activated satellite cells (myoblasts) and on myotubes during the regeneration process. As IGF-I and other growth factors have been implicated in satellite cell activity, it was important to ascertain what type of IGF-I may be involved.

For this purpose, local mechanical damage was induced by electrical stimulation of stretched muscles, mimicking a type of damage that occurs during eccentric muscle contraction. In another series of experiments, damage was induced by a myotoxic agent to determine if damage *per se*, as well as mechanical stress, would up-regulate those factors implicated in satellite cell activation. As satellite cells initially proliferate and then fuse with damaged fibres, a change in expression of certain adherins occurs. Their nuclei become reprogrammed to express muscle genes, and therefore M-cad and MyoD were chosen as marker genes to monitor this genetic reprogramming of the satellite cells *in vivo*.

As tissue repair is a local and continuing process throughout life, it is essential to use morphological methods to assess in which cell type the relevant genes are expressed and how this relates to the damaged area. In a complementary study (Hill & Goldspink, 2003) we have evaluated gene expression using real time RT-PCR, which permitted quantitative measurements in single rat muscles subjected to muscle damage. It was felt, however, that this present study should involve a more morphological examination of the muscle repair *in vivo*. The initiation of the IGF-I isoform expression could then be correlated with the appearance and distribution of satellite cell markers to establish which forms of IGF-I are likely to be involved in satellite cell activation.

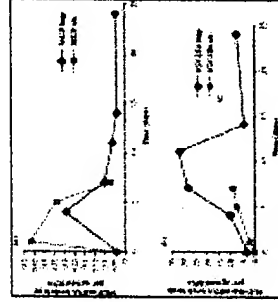
Materials and methods

Go to:



[Full Size]

Fig. 2 (a) Mean percentage of damaged-regenerating muscle fibre area in relation to the whole muscle se...



[Full Size]

Fig. 3 mRNA levels of MGF and IGF-IEa isoforms in the two models of muscle damage. MGF was maximally e...

[Choose]   Go

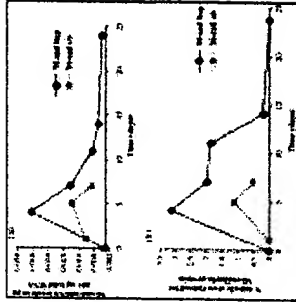
Induction of local muscle damage

Bupivacaine protocol for local muscle damage and repair

Sprague-Dawley rats, 250-300 g in body weight and 10-12 weeks of age, were divided equally into five experimental and two control groups ($n = 6$). The latter included untreated animals plus a sham control group injected with saline only. Young animals were studied because they have a greater potential for muscle regeneration than older subjects (Schultz & Lipton, 1982). Anaesthesia in the experimental and sham control animals was induced with approximately 3% halothane in oxygen at a flow rate of 2 L min^{-1} and subsequently maintained at ~1-2%. The left hind quarter was shaved to disclose the tibialis anterior (TA) and a 0.3-mL injection of either 0.5% bupivacaine hydrochloride (1-Butyl-N-[2,6-dimethylphenyl]-2-piperidine carboxamide Hydrochloride; Sigma) in 0.9% sodium chloride, or 0.9% sodium chloride only, was made into the middle of the TA muscle. A 26-gauge \times 13-mm-length needle was introduced at the midpoint of the muscle, inserted at an angle and advanced proximally along the muscle's longitudinal axis. The needle was then slowly withdrawn as the muscle expanded. In addition to sampling the contralateral muscle, controls included animals injected with physiological saline only, as well as normal rats of the same age and weight, which received no injection. Animals regained consciousness 10-15 min later. Regular checks were made to ensure rats were not in pain during the recovery period. The experimental animals were killed at intervals up to 25 days and the muscle used for morphological analysis as well as the determination of the corresponding mRNA levels.

Local muscle damage induced by the stretch combined with electrical stimulation

Sprague-Dawley rats, 250-300 g in body weight and 10-12 weeks of age, were divided into three experimental and two control groups. The TA of three groups of six rats was subjected to continuous stretch in the extended position with 1 h of stimulation of the peroneal nerve at a frequency of 30 Hz on days 1, 5 and 7 while the animals were anaesthetized. Six sham-operated controls, in which electrode wires were inserted near the peroneal nerve but the electrical stimulation circuit was not switched on, were also used. A further group of six rats subjected to no stretch or stimulation were used as normal controls. In all groups, muscle from the contralateral limb was also examined and served as a subgroup control. In the experimental and sham-operated animals, anaesthesia was induced as before and the left hindquarter of the hind limb was immobilized in plantar flexion using a fibreglass cast. Care was taken to ensure that blood flow to the foot was not compromised by omission of plaster cast around the ankle and by placing a cotton bud on the hind limb to ensure casting was not too tight. Electrical stimulation involved introducing stainless steel electrodes on either side of the peroneal nerve that were attached to a microstimulation circuit. When activated, the stimulators



[Full Size]

Fig. 4 M-cad mRNA and protein expression in damaged TA muscle following stretch and stimulation and bu...



[Full Size]

Fig. 5 M-cad staining in a cross-section of TA muscle (a) 4 days after bupivacaine injection, (b) 5 days...

To cite this article

Hill, Maria, Wernig, A. & Goldspink, G. (2003)

Muscle satellite (stem) cell activation during local tissue injury and repair.

Journal of Anatomy 203 (1), 89-99.

doi: 10.1046/

j.1469-7580.2003.00195.x

delivered bi-directional pulses of 1-ms duration, supramaximal intensity (3 V) at a frequency of 30 Hz (protocol taken from McKoy et al. 1999; altered and adjusted to the present model). At the end of stimulation, absorbable sutures (VICRYL 4/0) were used to close the incision and 0.3 mL of an analgesic (Tamgesic) was given subcutaneously. Animals regained consciousness 10–15 min later and the plaster cast still remained in position until the animals were killed. Regular checks were made to ensure that there was no swelling of the limb due to tight casting and that sutures were still in place. To analyse for morphological aspects of this type of local damage, muscles from these animals were killed at three time points up to 7 days and again used for the expression of certain morphological markers as well as their mRNA levels.

Tissue preparation

At the time points stated above for both studies, animals were killed using CO₂ and death was ensured by cervical dislocation. In the bupivacaine study, the TA muscle from both hind limbs was quickly removed, weighed under cold conditions and cut into two parts. One section of the TA was taken from the mid-belly region, covered in cryo-preserved (Tissue-Tek II, OCT Compound), snap-frozen by immersion in isopentane that had been cooled by liquid nitrogen and stored at –70 °C until further processing. Remaining TA muscle was processed for total RNA isolation. In the stretch and stimulation study, one part was taken from the distal tendon end and the other from the mid-belly region and processed as described above.

Assessment of muscle fibre damage and repair

Histological assessment

Cryostat sections were prepared and some of these were stained using the conventional H&E method and the area of damage determined using image analysis.

Expression of embryonic myosin

The primary monoclonal antibody to the embryonic myosin heavy chain (emb. MyHC) was used as a marker of muscle regeneration. The MyHc330 and secondary antibodies were a gift from A. F. M. Moorman (Anatomy and Embryology Department, AMC, Amsterdam). The established protocol was performed on gelatin-embedded single fibres and detection was based on an indirect unconjugated immunoperoxidase technique (PAP) according to Moorman et al. (1984). However, the protocol was modified to use biotin-streptavidin detection: sections were fixed for 5 min in a 4% (w/v) paraformaldehyde in 100 mM potassium phosphate buffer (pH 7.4), and washed twice in 150 mM NaCl, 50 mM Tris/HCl, pH 7.6 (TBS). Endogenous peroxidase activity was quenched by immersing the slides in 0.3% hydrogen peroxide (H₂O₂) in methanol for 20 min, using a shaker.

Sections were pre-incubated in a mixture of 5% horse serum, 0.5% Triton X-100 in TBS for 1 h at room temperature in a humidified chamber, before incubation with the emb. MyHC330 monoclonal antibody at room temperature overnight. This was followed by washing three times in TBS for 5 min and incubation with a horse antimouse secondary antibody (rat adsorbed) diluted 1 : 200 in 5% horse serum in TBS for 90 min at room temperature. Slides were washed three times for 5 min each in PBS, then incubated with ABC peroxidase reagent (Vector Laboratories kit) for 30 min at room temperature, washed three times for 5 min in PBS and the immunocomplex visualized by incubation with DAB substrate (Vector Laboratories kit) for 5 min. The colour reaction was stopped by washing sections in water and, following dehydration in ethanol washes of 50, 75, 90 and 100%, sections were mounted using DPX mounting medium (BDH).

M-cad used for identification of satellite cell marker proteins

M-cad rabbit polyclonal primary antibody was used according to a protocol based on that of Irintchev et al. (1994). Sections of 6 μm thickness were fixed in methanol for 4 min at 4 °C. Blocking solution of 20% normal goat serum (NGS) in PBS was applied for 30 min at room temperature in a humidified chamber. The solution was aspirated from sections before they were incubated at 4 °C overnight with M-cad primary antibody (produced by Professor Wernig's laboratory). This was diluted 1 : 50 in PBS containing 0.7% lambda carrageenan (Sigma) and 0.02% sodium azide. Following washing in PBS, sections were pre-incubated with 20% NGS diluted in PBS for 30 min to enhance specificity prior to incubation with a biotin-conjugated goat antirabbit secondary antibody (Jackson Immunoresearch Laboratories) diluted 1 : 200 in PBS-carrageenan solution for 1 h at room temperature. After washes in PBS, a fluorescein (DTAF)-conjugated streptavidin antibody (Jackson Immunoresearch) diluted 1 : 200 in PBS was applied for 30 min at room temperature. Sections were washed in PBS. To confirm the localization of the putative satellite cells, additional staining of nuclei with bis-benzimide and laminin with blue fluorescence was used to reveal the basal lamina. Following the last wash to remove M-cad secondary fluorescein antibody, sections were incubated with mouse antihuman laminin monoclonal antibody (Chemicon), diluted 1 : 1000 in PBS-carrageenan solution, for 1 h at room temperature. After three 5-min washes in PBS, a secondary antimouse Texas Red-labelled antibody (Molecular Probes), diluted 1 : 200 in PBS, was incubated for 45 min at room temperature. Following washing in PBS, 1 $\mu\text{g mL}^{-1}$ of bis-benzimide (Hoechst 33258, Sigma) diluted in PBS was incubated for 5 min to stain nuclei. Washed sections were then mounted in Fluoromount (Agar Scientific).

Image analysis

Images were acquired on a Nikon TE300 inverted microscope with fluorescent attachment (Nikon) and Photonic Science low-light-level, peltier-cooled, CCD camera (Photonic Science), controlled by Kontron KS400 image analysis software (Zeiss Microscience). In order to analyse the total percentage damage/regeneration with H&E staining, whole muscle sections were scanned under bright-field

conditions at 10x magnification using a motorized XY-stage (Prior) mounted on the Nikon inverted microscope and controlled by the KS400 image analysis software. Thereby, multiple microscope fields were collected (up to 10 x 10 fields) using the montage macro of the KS400 image analysis software to produce large montages of the whole muscle section. From these montages the areas lacking organized cellular structure could be delineated. For M-cad-specific staining, a minimum of five random fields per section containing a maximum of 100 muscle fibres were acquired from three sections per slide, over four slides at 20x magnification using fluorescence illumination with standardized imaging conditions for all specimens. Image analysis and H&E staining was performed using a custom-written KS400 macro program that allowed the user interactively to draw around damaged muscle fibres and express the identified area as a percentage of the total muscle area. It was apparent that there was some staining in the control sections as well as background fluorescence and the levels of detection were adjusted to remove this baseline staining. At higher magnifications than those used for image analysis, the fluorescence M-cad protein antibody complex was seen to be located mainly around the periphery of the muscle fibres and was detected even in the sections of the control muscles, but at a much lower level. Image analysis of the percentage increase in M-cad-positive staining was assessed by a semi-automatic segmentation macro, which allowed some limited interaction by the operator and expressed the results as AREA% of positive M-cad staining over the identified field.

RNA isolation and real-time RT-PCR

The single-step method of RNA isolation using acid guanidinium thiocyanate-phenol-chloroform after Chomczynski & Sacchi (1987) was used to isolate total RNA, from muscles that were used for morphological analysis. RNA concentrations were measured in a Genespec instrument (Shimadzu). First-strand cDNA synthesis for RT-PCR was performed using a Roche Diagnostics kit and cDNA samples were stored at -20 °C until required. In specific cDNA synthesis reactions, i.e. for MGF RT-PCR, 25 pmol of the sequence-specific primer MGF-rt was used in addition to the 25 pmol of random primers. Specific primers for IGF-1 α , MGF, MyoD and M-cad were used for the determination of these transcript levels as described in Owino et al. (2001) and Hill & Goldspink (2003). The RNA transcript levels for the different experimental and control muscles were analysed simultaneously and runs were carried out in triplicate. A negative control was present in each run where the template DNA was replaced with PCR-grade water. Briefly, reactions for the individual genes were optimized using SYBR Green I as the detection method and concentrations of the specific mRNAs given as picograms per microgram of total RNA as described in Owino et al. (2001) and Hill & Goldspink (2003).

Results

Go to:

Muscle wet weight post stretch and stimulation

Muscle weight

After 1 day of induced damage by stretch and stimulation, the TA muscle weight of both experimental and contralateral muscles remained approximately the same, as in the sham and normal control groups. After 5 days the TA muscle wet weight of the experimental limb was 11.6% less ($P < 0.001$) compared with the right contralateral TA and the 1-day group. Thereafter, the muscle weight increased again. Greater weight loss was evident in the bupivacaine-treated muscles ($\sim 33\%$ at 4 days) but by 24 days of recovery the muscle weight was significantly greater (10%) than for their contralateral controls ($P < 0.01$).

Time course and extent of morphological changes

Figure 1 shows examples of the sections that were stained for routine histological (H&E staining) and immunohistochemical (emb. MyHC) examination to assess local damage. None of the sham control muscles or contralateral muscles to the stretched and stimulated muscles showed any damage and were similar to the normal muscle group. Conversely, the bupivacaine-injected and the stretched/stimulated muscles showed extensive damage. Using the KS400 Image Analyser, it was found that in response to the bupivacaine insult (Fig. 2a) the percentage of damaged-regenerated area at day 4 was 67% and, thereafter, decreased gradually until day 24 when most of the muscle fibre architecture had returned to normal. Two-way ANOVA revealed that there were significant differences ($P < 0.05$) among the five time points concerning the duration of recovery of muscle fibres towards normal muscle morphology except between days 14 and 24.

Muscle repair following local damage was also confirmed by emb. MyHC labelling. This was absent from all muscle fibres in the control groups and the contralateral muscle of the bupivacaine-injected animals and normal muscle fibres that survived the bupivacaine insult. In agreement with the data from the mean percentage of damaged-regenerating area shown with the H&E analysis, the mean percentage of embryonic myosin-positive muscle fibres declined after 4 days to reach zero at 24 days (Fig. 2b).

Interestingly, the degree of damage in the stretched/stimulated muscles was found to be higher in the distal parts of the muscle than those in the middle of the muscle. Both show maximum areas of damage at 5 days with the myotendon end exhibiting an area of damage of 50% and the middle region 30%. Two days later the damage area had reduced to 30% in sections from the myotendon region and almost to zero for the middle region. The difference between the regions was also reflected in embryonic MyHC expression, with 90% of the muscle fibres in the distal region and 70% of the muscle fibre showing expression, and at 7 days there was a reduction to 50% expressing emb. MyHC.

Bupivacaine-treated TA muscles exhibited a sequence of degenerative and regenerative changes. At 4 days after bupivacaine injection, most of the muscle

fibres had degenerated, except from the periphery where muscle fibres were still intact. Macrophages filled areas of necrosis in which ghost-like remnants of the original fibres could occasionally be seen. The remaining fibres displayed features indicative of partial damage: a circular shape and 'moth-eaten' appearance, hyaline cytoplasm and pyknotic (but peripheral) myonuclei. However, dispersed colonies of regenerative fibres with central myonuclei could also be seen amongst the necrotic and normal fibres. At 7 days, a substantial fraction of the fibre population consisted of small regenerating fibres with peripheral nuclei migrating to the centre (defined as fibres that had an area less than 50% of the average for control muscle fibres) and many with central myonuclei as seen with the H&E stain. These fibres were larger than at day 4 and most of them reacted strongly with the emb. MyHC antibody. On day 11, regenerating fibres were larger and the number of these with central myonuclei and embryonic myosin-positive fibres was still large. After 14 days, the regenerating fibres were larger compared with those at 7 and 11 days. In addition, the reaction with emb. MyHC antibody had decreased compared with that at 11 days. Finally, on day 24, the fibre differentiation and morphology appeared normal and most of the myonuclei were now located at the periphery.

Time course of MGF and IGF-IEa expression

The mRNA levels of the two types of IGF-I at different time intervals are shown in Fig. 3(a,b). From Fig. 3(a) it can be seen that MGF expression had peaked by the first measurement at 1 day in the case of mechanical damage and 4 days following bupivacaine injection. By contrast, the expression of IGF-IEa (Fig. 3b) was much slower and took 12 days to peak following bupivacaine injection. In the case of mechanical damage, IGF-IEa was still rising at 7 days whereas MGF mRNA levels had already declined to their original (non-damaged) control levels by this time.

Expression of M-cad in stretched and stimulated TA muscle

M-cad mRNA also peaked surprisingly early at 5 days following damage (Fig. 4a). This was also the time for maximal expression of M-cad protein (Fig. 4b). Therefore, both M-cad mRNA and protein declined rapidly, indicating that satellite cell activation occurs within a relatively short period. M-cad antibody labelled small muscle fibres in a ring-like shape (Fig. 5) in damaged-regenerated muscle sections in response to stretch and stimulation. The reaction product was confined to the plasma membrane and never observed in the cytoplasm. Double labelling with laminin, a major component of the basal lamina of muscle fibres, was performed to determine the location of cells expressing M-cad. M-cad-positive cells are deemed to be muscle satellite cells contained within the basal lamina of muscle fibres and between this and the plasma membrane. The M-cad immunoreactivity in the stretched and stimulated muscle was associated with the damage-regeneration phase. One day following stretch and stimulation, no significant changes in the muscle morphology were observed. However, after 5 days the muscle sections in which there was marked inflammatory response and regeneration showed strong M-cad staining beneath the basal lamina of small regenerating fibres. This was very noticeable at the tendon region 7 days after injury, where regenerating fibres close

to the tendon demonstrated strong M-cad staining localized inside the laminin-positive fibres but the overall staining was less compared with that on day 5. In sham-operated control and normal muscle, no increase of M-cad expression was evident.

Discussion

Go to: 

The aim of the work described was to investigate the role of two IGF-I splice variants under conditions of damage and further regeneration of skeletal muscle. The application of highly sensitive PCR technology enabled amplification of low-abundance transcripts for the quantitative analysis of the locally produced insulin-like growth factors in muscle. During regeneration of skeletal muscle in young rats following ischaemia- or myotoxin-induced damage, elevated expression of IGF-I has been reported (Jennische & Hansson, 1987; Jennische et al. 1987; Edwall et al. 1989), which was diminished by day 15 of recovery (Marsh et al. 1997). However, the present study is the first to look at the distinct IGF-I isoforms, IGF-IEa and MGF, under such conditions and relate this to the activation of muscle satellite (stem) cells *in vivo*.

Results of the experiment in which damage was induced by bupivacaine demonstrated a surge of IGF-IEa mRNA expression that was maximal at 11 days and diminished thereafter to similar levels as those in the non-injected animals. By contrast, MGF mRNA showed a much earlier transient response that peaked at 4 days post bupivacaine injection and decreased thereafter, following mechanical damage, MGF peaked even earlier. It seems that in both myotoxin- and mechanical activity-induced damage models the temporal expression pattern for each IGF-I splice variant showed similar differential gene splicing sequences, with MGF peaking before IGF-IEa. This temporal difference in expression of the two muscle IGF-I RNA transcripts has also been described in the rat following commencement of resistance exercise (Adams, 2002). As M-cad expression peaked well before IGF-IEa, whether it was measured as mRNA or protein, it is unlikely that the systemic type of IGF-IEa is responsible for initial activation of satellite cells. However, it is not possible to determine from these data whether this was due to an increase in number of satellite cells because it is known that quiescent satellite cells do stain to some extent for M-cad protein (Rosenblatt et al. 1999). Nevertheless, this does represent a marked increase of M-cad, whether in existing satellite cells or an increase in the number of these cells or both.

MGF and IGF-IEa splice variants apparently yield the same mature peptide, which is derived from the highly conserved exons 3 and 4 of the IGF-I gene. These exons present in all the known IGF splice variants are known to code for the IGF-I receptor ligand domain. A mechanism of extracellular endoproteolysis of the IGF-I pro-hormone results in the same mature peptide (Gilmour, 1994), even though the splice variants of IGF-I may have different 3' sequences including the E domain. It has been suggested that IGF-I precursors could be pluripotent, in a form analogous to that of pro-hormone proopiomelanocortin and proglucagon (Siegfried et al. 1992).

The observation that a synthetic peptide derived from the rat Eb domain induces proliferation in epithelial cells is noteworthy (Siegfried et al. 1992). The role of the growth-promoting properties of the E peptide in MGF, acting as an independent growth factor, is supported by the recent cell culture experiments of Yang & Goldspink (2002), in which stable transfection with MGF was shown to stimulate myoblast proliferation but differentiation was suppressed. The addition of a synthetic MGF peptide or the medium from MGF-transfected cells onto normal C2C12 cells also inhibited their differentiation. Yet this inhibition was reversed when the peptide or the medium were withdrawn. By contrast, cells of the liver type of systemic IGF-I (IGF-IEa)-positive clone did form myotubes and the normal cell lines showed less cellular proliferation as well as forming myotubes. Of particular interest was the observation that when an IGF-I receptor antibody was added to the muscle cell cultures, cell proliferation induced by MGF was not inhibited whereas their stimulation to increase in mass and to form myotubes by IGF-I was repressed. This result strongly suggests that MGF is involved in another signalling pathway in addition to that associated with the IGF-I receptor.

As satellite cells appear to play an important role in muscle repair and adaptation it was important to investigate the expression of a satellite cell marker under conditions of damage and regeneration and to relate this to the temporal expression of the mechanosensitive MGF and/or the systemic type IGF-IEa. One of the most useful and suitable markers for the identification of satellite cells for this work proved to be the cell surface protein M-cad, because it has been shown to play a significant role in alignment and fusion of myoblasts to form and expand developing myotubes (Cifuentes-Diaz et al. 1995) and has been detected in satellite cells of normal muscle and during regenerative responses after muscle damage (Moore & Walsh, 1993; Irintchev et al. 1994). The early and acute surge of MGF mRNA following mechanical and myotoxic damage in this study strongly suggests that it is this splice variant of IGF-I that is involved in initiating the proliferation and differentiation of satellite cells. M-cad expression had already peaked when damage was evident, i.e. at 4 days post bupivacaine injection (Fig. 4a,b) and 5 days post stretch and stimulation (Figs 2a and 4b), and started to decrease once regeneration, fusion of myoblasts, had begun. The mRNA results were confirmed by the presence of M-cad protein in the activated satellite cells of the damaged muscles. This was very evident at 5 days by antibody staining (Fig. 5), and its RNA levels were seen to peak by 4 days following bupivacaine injection in the stretch and stimulation model (Fig. 4a). As MGF expression precedes M-cad mRNA and protein expression, this strongly suggests that this splice variant rather than IGF-IEa is involved in satellite cell activation. The latter (IGF-IEa) is expressed and peaks at 10 days following the insult. Although IGF-IEa is probably not involved in the initial activation of satellite cells, it is important that the repair process continues after the initial events and IGF-IEa is expressed at higher levels than MGF and is therefore a greater source of the mature peptide (IGF-I ligand domain). IGF-IEa expression may therefore be regarded as the second phase of local tissue repair as it is necessary to maintain protein synthesis rates in order to restore muscle mass. A specific monoclonal antibody is being generated to the MGF peptide. This will, we hope, permit its expression to be studied and compared with that of the mature IGF-I peptide, which is encoded by the RNA of both splice variants expressed in muscle following damage.

The results of these studies provide additional insight into the complexity of the IGF-I system and its implications under conditions of damage and subsequent regeneration. IGF-IEa and MGF are produced by active muscle in rodents and have been shown to be positive regulators of muscle hypertrophy (Goldspink, 1999; McKay et al. 1999; Owino et al. 2001). However, as reported here, the MGF isoform is acutely induced, whereas IGF-IEa has a delayed effect that is sustained during the later phase of regeneration. When comparing mechanical damage with myotoxin damage it is apparent that both involve a relatively rapid expression of the MGF splice variant, although it may seem that this growth/repair factor has been misnamed 'mechanogrowth factor'. However, even in the case of myotoxin damage it is likely that the damaged tissue mass is subjected to increased mechanical strain that results in the same cellular response. As the expression of the autocrine splice variant (MGF) precedes satellite cell activation, it is likely that this form of IGF-I is associated with satellite cell activation, not the systemic IGF-IEa type. This is in accord with the finding that MGF is not expressed in dystrophic muscles (Goldspink et al. 1996) and the decrease in MGF mRNA levels in response to mechanical overload in older muscles (Owino et al. 2001). There is a deficiency of active satellite cells in both these situations, in which local tissue repair becomes increasingly impaired. Experiments to investigate the expression of the two transcripts and activation of satellite cells in young and old muscles after the therapeutic application of MGF and IGF-IEa to ameliorate muscle loss are in progress.

Ackn w/ dgments

Go to:

Choose

Go

During this study M.H. received a PhD research studentship from the Anatomical Society of Great Britain and Ireland. Professor Goldspink also received support from the Wellcome Trust, the International Olympic Games WADA Committee and an EC (PENAM) grant for studying the effects of exercise including muscle damage. We are grateful to Dr Chris Thrasivoulou for his help with image analysis and Dr Jenny Weaden for her helpful comments on the manuscript.

References

Go to:

Choose

Go

Adams GR (1998) Role of insulin-like growth factor-I in the regulation of skeletal muscle adaptation to increased loading. *Exerc. Sport Sci. Rev.* **26**, 31-60.

[MEDLINE](#) [ISI/Abstract](#)

Adams GR (2002) Exercise effects on muscle insulin signalling and action. Invited Review: Autocrine/paracrine IGF-I and skeletal muscle adaptation. *J. Appl. Physiol.* **93**, 1159-1167.

[MEDLINE](#) [ISI/Abstract](#)

Aziz-Ullah, Goldspink G (1974) Distribution of mitotic nuclei in the biceps brachii

of the mouse during post-natal growth. *Anat. Rec.* **179**, 115-118.

MEDLINE

Beauchamp JR, Heslop L, Yu DS, Tajbakhsh S, Kelly RG, Wernig A, *et al.* (2000) Expression of CD34 and Myf5 defines the majority of quiescent adult skeletal muscle satellite cells. *J. Cell Biol.* **151**, 1221-1234.

CrossRef

MEDLINE

ISI Abstract

Bornemann A, Schmalbruch H (1994) Immunocytochemistry of M-cadherin in mature and regenerating rat muscle. *Anat. Rec.* **239**, 119-125.

MEDLINE

ISI Abstract

CSA

Chakravarthy MV, Fiorotto ML, Schwartz RJ, Booth FW (2001) Long-term insulin-like growth factor-I expression in skeletal muscles attenuates the enhanced in vitro proliferation ability of the resident satellite cells in transgenic mice. *Mech. Ageing Dev.* **122**, 1303-1320.

CrossRef

MEDLINE

ISI Abstract

Chomczynski P, Sacchi N (1987) Single-step method of RNA isolation by acid guanidinium thiocyanate-phenol-chloroform extraction. *Anal. Biochem.* **1162**, 156-159.

CrossRef

MEDLINE

- Cifuentes-Diaz C, Nicolet M, Alameddine H, Goudou D, Dehaupas M, Rieger F, *et al.* (1995) M-cadherin localization in developing adult and regenerating mouse skeletal muscle: possible involvement in secondary myogenesis. *Mech. Dev.* **50**, 85-97.

CrossRef

MEDLINE

- Cohn RD, Campbell KP (2000) Molecular basis of muscular dystrophies. *Muscle Nerve* **23**, 1456-1471.

CrossRef

MEDLINE

ISI Abstract

Cornelison DD, Wold BJ (1997) Single-cell analysis of regulatory gene expression in quiescent and activated mouse skeletal muscle satellite cells. *Dev. Biol.* **191**, 270-283.

CrossRef

MEDLINE

ISI Abstract

CSA

De Angelis I, Berghella I, Coletta M, Lattanzi I, Zanchi M, Cusella Angelis MG, *et al.* (1999) Skeletal myogenic progenitors originating from embryonic dorsal aorta coexpress endothelial and myogenic markers and contribute to postnatal muscle growth and regeneration. *J. Cell Biol.* **147**, 869-878.

CrossRef

MEDLINE

ISI Abstract

Edwall D, Schalling M, Jennische E, Norstedt G (1989) Induction of Insulin-like Growth Factor-I messenger ribonucleic acid during regeneration of rat skeletal

muscle. *Endocrinology* **124**, 820-825.

MEDLINE ISI Abstract CSA

Ferrari G, Cusella-De Angelis G, Coletta M, Paolucci E, Stomaluolo A, Cossu G, *et al.* (1998) Muscle regeneration by bone marrow-derived myogenic progenitors. *Science* **279**, 1528-1530.

ISI Abstract MEDLINE CSA

- Gilmour RS (1994) The implications of insulin-like growth factor mRNA heterogeneity. *J. Endocrinol.* **140**, 1-3.

MEDLINE ISI Abstract CSA

Goldspink G, Yang SY, Skarli M, Vrbova G (1996) Local growth regulation is associated with an isoform of IGF-I that is expressed in normal muscles but not in dystrophic muscles when subjected to stretch. *J. Physiol.* **495**, 162.

Goldspink G (1999) Changes in muscle mass and phenotype and the expression of autocrine and systemic growth factors by muscle in response to stretch and overload. *J. Anat.* **194**, 323-334.

MEDLINE ISI Abstract

Griffin G, Williams P, Goldspink G (1971) Region of longitudinal growth in striated muscle fibres. *Nature New Biol.* **232**, 28-29.

MEDLINE

Grounds MD (1998) Age-associated changes in the response of skeletal muscle cells to exercise and regeneration. *Ann. NY Acad. Sci.* **854**, 78-91.

MEDLINE ISI Abstract

- Haddad F, Adams GR (2002) Selected contribution: acute cellular and molecular responses to resistance exercise. *J. Appl. Physiol.* **93**, 394-403.

MEDLINE ISI Abstract

Hill M, Goldspink G (2003) Expression and splicing of the insulin-like growth factor gene in rodent muscle is associated with muscle satellite (stem) cell activation following local tissue damage. *J. Physiol.* **549**, 409-418.

Irintchev A, Zeschnick M, Starzinski-Powitz A, Wernig A (1994) Expression pattern of M-cadherin in normal, denervated and regenerating mouse muscle. *Dev. Dyn.* **199**, 326-337.

MEDLINE ISI Abstract

Jennische E, Hansson HA (1987) Regenerating skeletal muscle cells express insulin-like growth factor I. *Acta Physiol. Scand.* **130**, 327-332.

MEDLINE ISI Abstract CSA

Jennische E, Skottner A, Hansson HA (1987) Satellite cells express the trophic

factor IGF-I in regenerating skeletal muscle. *Acta Physiol. Scand.* **129**, 9-15.

MEDLINE ISI Abstract CSA

- Lieber RL, Friden J (1999) Mechanisms of muscle injury after eccentric contraction. *J. Sci. Med. Sport* **2**, 253-265.

MEDLINE

Marsh DR, Criswell DS, Hamilton MT, Booth FW (1997) Association of IGF-I mRNA expressions with muscle regeneration in young, adult, and old rats. *Am. J. Physiol.* **273**, R353-R358.

MEDLINE CSA

Mauro A (1961) Satellite cells of skeletal muscle fibres. *J. Biophys. Biochem. Cytol.* **9**, 493-495.

McKoy G, Ashley W, Mander J, Yang SY, Williams N, Russell B, et al. (1999) Expression of insulin-like growth factor-I splice variant and structural genes in rabbit skeletal muscle induced by stretch and stimulation. *J. Physiol.* **516**, 583-592.

MEDLINE ISI Abstract

Moore R, Walsh FS (1993) The cell adhesion molecule M-cadherin is specifically expressed in developing and regenerating, but not denervated skeletal muscle. *Development* **117**, 1409-1420.

MEDLINE ISI Abstract

Moorman AFM, de Boer PAJ, Linders M, Charles R (1984) The histone H5 variant in *Xenopus laevis*. *Cell Differ.* **14**, 113-123.

MEDLINE

Moss FP, Leblond CP (1970) Satellite cells as the source of nuclei in muscles of growing rats. *Anat. Rec.* **170**, 421-435.

MEDLINE ISI Abstract

Owino V, Yang SY, Goldspink G (2001) Age-related loss of skeletal muscle function and the inability to express the autocrine form of insulin-like growth factor-1 (MGF) in response to mechanical overload. *FEBS Lett.* **505**, 259-263.

MEDLINE ISI Abstract

Pye D, Watt DJ (2001) Dermal fibroblasts participate in the formation of new muscle fibres when implanted into regenerating normal mouse muscle. *J. Anat.* **198**, 163-173.

MEDLINE ISI Abstract

Qu-Petersen Z, Deasy B, Jankowski R, Ikezawa M, Cummins J, Pruchnic R, et al. (2002) Identification of a novel population of muscle stem cells in mice.

potential for muscle regeneration. *J. Cell Biol.* **157**, 851-864.

Rosenblatt JD, Cullen MJ, Irintchev A, Wernig A (1999) M-cadherin is a reliable molecular marker of satellite cells in mouse skeletal muscle. *Eur. J. Physiol.* **437**, R145.

Schultz E, Lipton BH (1982) Skeletal muscle cells: changes in proliferation potential as a function of age. *Mech. Ageing Dev.* **20**, 337-383.

Schultz E (1996) Satellite cell proliferative compartments in growing skeletal muscles. *D. v. Biol.* **175**, 84-94.



Seale P, Rudnicki MA (2000) A new look at the origin, function and 'stem-cell' status of muscle satellite cells. *Dev. Biol.* **106**, 115-124.

Siegfried JM, Kasprzyk PG, Treston AM, Mulshine JL, Quinn KA, Cuttitta F (1992) A mitogenic peptide amide encoded within the E peptide domain of the insulin-like growth factor IB prohormone. *Proc. Natl Acad. Sci. USA* **89**, 8107-8111.





Tabary JC, Tabary C, Tardieu G, Goldspink G (1972) Physiological and structural changes in the cat's soleus muscle due to immobilization at different lengths by plaster casts. *J. Physiol.* **224**, 231-244.

Wernig A, Irintchev A, Weisshaupt P (1990) Muscle injury, cross-sectional area and fibre type distribution in mouse soleus after intermittent wheel-running. *J. Physiol.* **428**, 639-652.

Williams P, Goldspink G (1971) Longitudinal growth of striated muscle fibres. *J. Cell Sci.* **9**, 751-767.

Williams PE, Goldspink G (1976) The effect of denervation and dystrophy on the adaptation of sarcomere number to the function length of the muscle in young and adult mice. *J. Anat.* **122**, 455-465.

Yang SY, Alnaqeeb M, Simpson H, Goldspink G (1996) Cloning and characterisation of an IGF-I isoform expressed in skeletal muscle subjected to stretch. *J. Muscle Res. Cell Motility* **17**, 487-495.

MEDLINE ISI/Abstract

Yang SY, Goldspink G (2002) Different roles of the IGF-IEc peptide (MGF) and mature IGF-I in myoblast proliferation and differentiation. *FEBS Lett.* **522**, 156-160.

CrossRef

MEDLINE

ISI Abstract

Journal of Anatomy

Volume 203 Issue 1 Page 89 - July 2003

Blackwell Synergy® is a Blackwell Publishing, Inc. registered trademark
More information about Blackwell Synergy - online journals from www.blackwellpublishing.com.
We welcome your Feedback. See our [Privacy Statement](#) and [Terms and Conditions](#).
Technology Partner - [Atypoon Systems, Inc.](#)



letters to nature

Nature 425, 968 - 973 (30 October 2003); doi:10.1038/nature02069

Nature AOP, published online 12 October 2003

Fusion of bone-marrow-derived cells with Purkinje neurons, cardiomyocytes and hepatocytes

MANUEL ALVAREZ-DOLADO¹, RICARDO PARDAL², JOSE M. GARCIA-VERDUGO³, JOHN R. FIKE¹, HYUN O. LEE², KLAUS PFEFFER⁴, CARLOS LOIS⁵, SEAN J. MORRISON² & ARTURO ALVAREZ-BUYLLA¹

¹ Department of Neurological Surgery, University of California at San Francisco, San Francisco, California 94143-0520, USA

² Howard Hughes Medical Institute, Department of Internal Medicine, University of Michigan, Ann Arbor, Michigan 48109-0934, USA

³ Instituto Cavanilles, University of Valencia, Valencia 46100, Spain

⁴ Institute of Medical Microbiology, University of Dusseldorf, D-40225 Dusseldorf, Germany

⁵ Picower Center for Learning and Memory, Massachusetts Institute of Technology, Cambridge, Massachusetts 02139-4307, USA

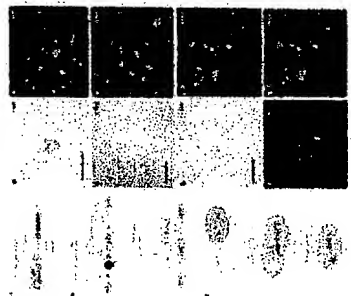
Correspondence and requests for materials should be addressed to A.A.-B. (abuylla@itsa.ucsf.edu).

Recent studies have suggested that bone marrow cells possess a broad differentiation potential, being able to form new liver cells, cardiomyocytes and neurons^{1, 2}. Several groups have attributed this apparent plasticity to 'transdifferentiation'³⁻⁵. Others, however, have suggested that cell fusion could explain these results⁶⁻⁹. Using a simple method based on Cre/lox recombination to detect cell fusion events, we demonstrate that bone-marrow-derived cells (BMDCs) fuse spontaneously with neural progenitors *in vitro*. Furthermore, bone marrow transplantation demonstrates that BMDCs fuse *in vivo* with hepatocytes in liver, Purkinje neurons in the brain and cardiac muscle in the heart, resulting in the formation of multinucleated cells. No evidence of transdifferentiation without fusion was observed in these tissues. These observations provide the first *in vivo* evidence for cell fusion of BMDCs with neurons and cardiomyocytes, raising the possibility that cell fusion may contribute to the development or maintenance of these key cell types.

In order to detect cell fusion we used a method based on Cre/lox recombination, a technique extensively used to conditionally turn on or off gene expression in specific cell types or tissues, or at particular stages in development¹⁰. For this study we first used mice expressing Cre recombinase ubiquitously under the control of a hybrid cytomegalovirus (CMV) enhancer β -actin promoter¹¹ (Fig. 1a), and the conditional Cre reporter mouse line R26R¹² (Fig. 1b). In this line, the LacZ reporter gene is exclusively expressed after the excision of a loxP-flanked (floxed) stop cassette by Cre-mediated recombination (Fig. 1b). When Cre-expressing (Cre⁺) cells fuse with R26R cells, Cre recombinase excises the floxed stop cassette of the reporter gene in the R26R nuclei, resulting in expression of LacZ in the fused cells. Consequently, fused cells can be detected easily by 5-bromo-4-chloro-3-indolyl- β -D-galactoside (X-gal) staining (Fig. 1c). This method previously failed to detect

evidence of cell fusion in the pancreas¹³. For this reason, we first verified this cell fusion detection method *in vitro*.

Figure 1 Method to detect cell fusion events.



High resolution image and legend (81k)

We co-cultured bone marrow stromal cells (BMSCs) from R26R reporter mice with Cre⁺ multipotent progenitor cells isolated from postnatal brain and grown as neurospheres¹⁴. Previous studies have shown that these two cell types can fuse with embryonic stem cells *in vitro*^{6,7}. After 4 days *in vitro* (DIV), a small proportion of β-gal⁺ cells were found in these co-cultures (1 to 2 cells per 80,000 cells) (Fig. 1d). Importantly, most β-gal⁺ cells at 4 DIV had two or more nuclei, an observation that was confirmed by electron microscopy (Fig. 1e, i; see also Supplementary Fig. 1). This is consistent with the generation of β-gal⁺ cells by fusion. Notably, after 10 or 15 DIV β-gal⁺ cells formed small colonies and some of these cells were mitotic (Fig. 1g and inset). Cells in these colonies were invariably mononucleated, suggesting that with time and cell division the nuclei of these cells fuse or supernumerary nuclei are eliminated. In addition to neurosphere cells, R26R BMSCs were also co-cultured with primary cultures of Cre⁺ fibroblasts. Three independent co-cultures did not yield positive cells, suggesting that not all cell types are equally capable of fusion in culture. To further confirm that β-gal expression was due to cell fusion, Cre⁺ neurosphere cells were labelled with 5-bromodeoxyuridine (BrdU) and then co-cultured for 5 days with R26R BMSCs. Most bi-nucleated β-gal⁺ cells in these cultures had only one of the two nuclei labelled with BrdU (Fig. 1h–k), further confirming the reliability of this method to detect fusion events.

These results confirm previous work demonstrating that cell fusion occurs spontaneously *in vitro*^{6,7}. To study cell fusion *in vivo*, R26R reporter mice were lethally irradiated, and 2 days later were grafted with bone marrow from mice constitutively expressing Cre recombinase and green fluorescent protein (GFP) under the control of the β-actin promoter (β-actin-Cre-GFP mice, see 'allogeneic bone marrow transplantation' section of Methods). We analysed the grafted mice at 2 (*n* = 3) and 4 (*n* = 3) months after transplantation. These mice showed significant levels of haematopoietic reconstitution, which was measured by flow cytometry based on the frequency of GFP⁺ cells in peripheral blood (from 54.6% to 79.8% of nucleated blood cells). Brain, liver, heart, gut, kidney, lung and skeletal muscle from these mice were serially sectioned and stained for the presence of X-gal⁺ cells. In all animals, cells labelled with β-gal were only found in brain, heart

and liver, and not in the other organs studied ([Table 1](#)). As a negative control, we grafted R26R mice with bone marrow from wild-type mice. We did not find β -gal⁺ cells in these animals, demonstrating that the reporter was not inappropriately activated, even after irradiation.

BMDs fuse with hepatocytes in fumarylacetoacetate-hydrolase-deficient mice^{8, 9}. Consistent with this finding, we also observed fused hepatocytes in our grafted mice ([Fig. 2](#)). β -gal⁺ hepatocytes expressed albumin (a characteristic hepatocyte marker) ([Fig. 2, h](#)) but were negative for CD45 (a haematopoietic marker) (data not shown). Electron microscopy confirmed that these fused cells were typical hepatocytes with no features of haematopoietic cells ([Fig. 2c](#)). They contained glycogen granules, complete desmosomes and bile canaliculi ([Fig. 2d](#)). Two months after transplant most β -gal⁺ hepatocytes co-expressed the donor marker GFP ([Fig. 2e, f](#)); however, a small fraction of fused hepatocytes were GFP negative. This fraction had increased 4 months after transplantation ([Table 1](#)). This result suggests that after fusion donor genes may be inactivated/eliminated over time.

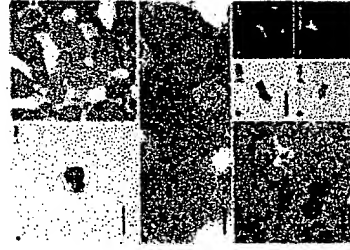


Figure 2 Fusion of hepatocytes with BMDs after bone marrow transplantation.

High resolution image and legend (119k)

At 2 and 4 months after transplantation, β -gal⁺ cells were detected in the cerebellum, where labelled cells displayed the typical location and morphology of Purkinje cells ([Fig. 3a](#)). Two β -gal⁺ cells were embedded in plastic and serially sectioned for light and electron microscopy. Serial reconstruction of the soma of these cells demonstrated the presence of two nuclei ([Fig. 3b](#); see also [Supplementary Fig. 2](#)). Notably, the two nuclei presented very different morphologies: one had a wrinkled surface with multiple invaginations and a single nucleolus, typical of Purkinje cells¹⁵, whereas the second nucleus showed a uniform spherical shape with multiple nucleoli, suggesting a different origin ([Fig. 3b, c](#)). Electron microscopy analysis confirmed that these cells were Purkinje neurons ([Fig. 3c](#)) with typical Purkinje cell somata and organelle distribution, including structures with the characteristics of synaptic contacts ([Fig. 3d](#)). No signs of degeneration or abnormal structures were observed in the cytoplasm of these cells ([Fig. 3c, d](#)). β -gal⁺ Purkinje cells stained positively for the Purkinje cell marker calbindin (data not shown). This is the first direct evidence, to our knowledge, showing that a neuron can fuse with a BMD. These results suggest that previous observations of small numbers of Purkinje cells bearing markers of transplanted bone marrow cells^{5, 16, 17} may have arisen by fusion rather than transdifferentiation.

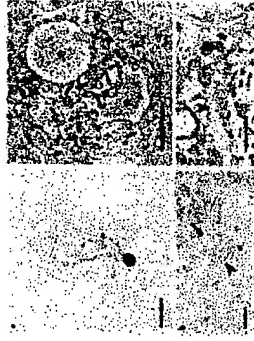


Figure 3 Purkinje cells fuse with BMDCs after bone marrow transplantation.

[High resolution image and legend \(74k\)](#)

The third organ where β -gal⁺ cells were found was the heart (Fig. 4). The β -gal⁺ cells were integrated into the myocardial wall and had a morphology and alignment that was indistinguishable from the surrounding cardiac muscle fibres (Fig. 4a–d). At the electron microscopy level, the fused cells had the morphology of mature cardiomyocytes, including developed filament bands and mature intercalated discs with desmosomes and GAP junctions connecting to neighbouring fibres (Fig. 4e). In addition, fused cardiomyocytes expressed cardiac troponin I (Fig. 4g). As seen in the liver, GFP was expressed in most of the fused cardiomyocytes at 2 months after transplantation (Table 1). In contrast, fused cardiomyocytes lost GFP expression at 4 months (Fig. 4h). It has been suggested that haematopoietic stem cells can partially restore the infarcted heart by transdifferentiation, giving rise to new myocardium⁴. Our results suggest that BMDCs can fuse with cells within the heart to form mature cardiomyocytes, but it remains unknown whether any new cardiomyocytes are generated as a result of this fusion.

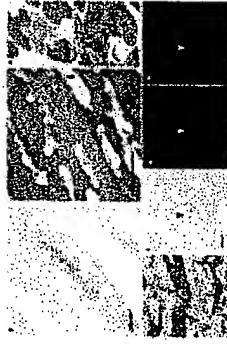


Figure 4 BMDCs fuse with cells in the heart.

[High resolution image and legend \(62k\)](#)

Bone marrow cells include haematopoietic cells as well as mesenchymal cells and possibly other cell types. To test whether haematopoietic cells were participating in fusion events *in vivo* we used donor mice in which Cre recombinase was knocked into the CD45 locus (CD45-Cre). As CD45 is specifically expressed by haematopoietic cells^{18, 19}, recombination should only occur in fusions involving cells of the haematopoietic lineage. To confirm the CD45-Cre expression pattern these mice were mated with R26R reporter mice. We observed widespread β -gal expression in haematopoietic stem cells, bone marrow cells, and blood cells but not in other tissues such as brain, liver, or skeletal muscle (Supplementary Fig. 3). Nonetheless, we cannot rule out the possibility of CD45-Cre expression by very rare cells in other tissues or that non-haematopoietic cells might transiently activate CD45 expression during whatever nuclear reprogramming might occur after cell fusion.

CD45-Cre bone marrow cells were injected into four lethally irradiated R26R mice to look for fusion events (see 'Congenic bone marrow transplantation' section of Methods). The engrafted mice were analysed 10 months after transplantation. Consistent with the above observations, we found β -gal⁺ hepatocytes in all four mice (Table 1; see also Supplementary Fig. 3e). β -gal⁺ cardiomyocytes were found in two of the four mice, and β -gal⁺ Purkinje cells were observed in one mouse (Table 1; see also Supplementary Fig. 3). As a negative control, we lethally irradiated seven R26R mice and transplanted them with 5×10^5 R26R bone marrow cells. No β -gal⁺ cells were observed in these mice. These experiments suggest that haematopoietic cells fuse *in vivo* with cells in liver, heart and brain, but this does not rule out the possibility that other types of BMDCs might also participate in fusion.

In R26R mice that had been transplanted with bone marrow cells from β -actin-Cre-GFP mice, we looked for evidence of transdifferentiation in the grafted animals. GFP⁺ cells that were negative for β -gal (that is, they did not fuse with recipient R26R cells) exhibited characteristics of microglia in the brain, of Kupffer or pit cells in the liver, and of macrophages in the heart (Supplementary Fig. 4). Each of these cell types are of haematopoietic origin²⁰⁻²² and can fuse under certain conditions²³, making them candidates for the haematopoietic cells that fused with resident cells. In contrast, no GFP⁺/ β -gal⁻ cells with the appearance of neural cells, hepatocytes, or cardiac muscle cells were observed. This suggests that cell fusion is the major mechanism by which haematopoietic cells can contribute to these tissues; however, our data do not rule out the possibility of rare transdifferentiation events, especially by other cell types or under other experimental conditions.

Our results suggest that BMDCs fuse with selective cell types in three organs. We did not observe evidence of fusion in skeletal muscle, gut, kidney, or lung in these experiments. The lack of evidence for fusion in these organs could be due to a lower efficiency of Cre-mediated recombination in these tissues or lower expression of the reporter gene (Supplementary Fig. 5). Alternatively, fusion may only occur in these tissues at a lower rate or under other experimental conditions, such as after injury.

With the exception of irradiation, the mice used in these experiments were healthy and did not have any pre-existing injury or pathology. Reconstitutions involving the β -actin-Cre-GFP mice were allogeneic and therefore could have experienced graft-versus-host injury. However, reconstitutions involving CD45-Cre mice were congenic and did not involve any histoincompatibility. Although qualitatively similar results were observed in both contexts, considerable variation was observed from mouse to mouse in the extent to which fusion was observed. Therefore, the efficiency of somatic fusion *in vivo* is probably influenced by many variables.

Our results raise the fundamental question of whether fusion between haematopoietic cells and cells of the brain, liver and heart has a physiological role in the development or maintenance of these organs. Interestingly, many hepatocytes and cardiomyocytes under normal conditions have two or more nuclei^{22, 24}. To our knowledge this is the first study to demonstrate Purkinje cells with two nuclei, but other studies have suggested that these neurons can be polyploid^{25, 26}. Our results suggest that cell fusion may be the mechanism by which these cells become multinucleated or polyploid. Genetic material derived from blood cells may contribute through cell fusion to the survival and function of cells in different organs. Previous studies have shown that fused cells are positively selected during hepatic degeneration, helping to rescue a mutant mouse deficient for fumarylacetoacetate hydrolase^{8, 9}. Our observation that fusion is a major mechanism by which BMDCs contribute to the heart, liver and brain draws into question the rationale for clinical procedures based on the idea that

transdifferentiation of BMDCs can lead to the *de novo* generation of heart or brain cells. Additional studies in animal models will be required to determine whether fusion by BMDC cells can be used in reparative cell therapy.

Methods

Cell cultures Bone marrow cells from β -actin-Cre or R26R transgenic mice were collected by flushing tibias and femurs with RPMI medium 1640 (Gibco BRL) supplemented with 3% fetal calf serum. Red blood cells were depleted using ice-cold ammonium chloride (140 mM in Tris 17 mM), and bone marrow cells were plated at a density of $2-4 \times 10^7$ cells per 9.5 cm^2 in Iscove's modified Dulbecco's medium (IMDM; Gibco BRL) supplemented with 10% fetal calf serum, 100 U ml^{-1} penicillin, 100 mg ml^{-1} streptomycin and 10 mg ml^{-1} glutamine (complete IMDM medium). The non-adherent cell population was removed after 48 h and the adherent BMDC layer washed once with fresh medium; cells were then continuously cultured for 1–4 weeks.

For neurospheres, brain subventricular zone from 5–10-day-old β -actin-Cre or R26R mice was collected. After papain dissociation, neurospheres were cultured and expanded in the presence of both epidermal growth factor (20 ng ml^{-1} ; Peprotech) and fibroblast growth factor-2 (10 ng ml^{-1} ; Peprotech), as described²⁷. For BrdU labelling, neurospheres were cultured for 15 min in the presence of 2 μM BrdU, washed, and expanded for two additional passages before being cultured with BMSCs. This procedure labelled 70–80% of the neurosphere cells. Fibroblasts were cultured as described previously²⁸.

Co-cultures BMDCs and dissociated neurospheres were mixed in a 1:1 ratio and plated on Matrigel-coated dishes (BD Bioscience) at a density of 2×10^5 cells ml^{-1} in complete IMDM medium. BMDCs and primary fibroblasts were cultured in a 1:1 ratio on plastic dishes in complete IMDM medium. After 4–15 days, co-cultures were washed and fixed in 2% paraformaldehyde for 10 min and analysed by X-gal staining or immunohistochemistry. As a negative control, R26R BMDC monocultures were grown for 15 days in the presence of conditioned medium or cell extracts from Cre-expressing cells (data not shown). Cell extracts from Cre-expressing cells were freshly prepared by two freeze/thaw series and added to the culture medium.

Animal care and bone marrow transplant Animal care and all procedures were approved by the Institutional Animal Care Committees at UCSF and the University of Michigan.

Allogeneic bone marrow transplantation Homozygous mice expressing Cre recombinase under the control of the hybrid regulatory element CMV enhancer β -actin promoter¹¹, and homozygous mice expressing GFP under the same promoter²⁹ were bred to generate β -actin-Cre-GFP mice for use as bone marrow donors. Bone marrow cells from 8–10-week-old Cre-GFP⁺ mice were extracted as described, and $10-20 \times 10^6$ cells were intraperitoneally injected into R26R mice irradiated with a single whole-body dose of 7.5 Gy. To avoid allograft rejection, mice that received the bone marrow transplantation procedure were treated one week before transplantation and 3 weeks after transplantation with Neoral cyclosporine (100 mg l^{-1} ; Novartis) in the drinking water. Drinking water was acidified and contained neomycin sulphate (1 mg l^{-1} ; Sigma) to suppress pathogens.

Congenetic bone marrow transplantation In an independent experiment 8–10-week-old CD45-Cre 'knock-in' mice on a C57BL/Ka-Thy1.1 background were used as donors of bone marrow cells. The generation of CD45-Cre knock-in mice will be described elsewhere (E. Schaller and K.P., manuscript in preparation). Eight-week-old R26R mice on a C57BL/Ka-Thy1.2 background were used as recipients. Approximately 5×10^5 bone marrow cells were injected into the retro-orbital venous plexus of R26R mice lethally irradiated with two doses of 5.7 Gy each. The drinking water of the transplanted mice contained neomycin sulphate (1 g l^{-1}) and polymyxin B sulphate ($1 \times 10^6 \text{ U l}^{-1}$) to suppress pathogens. On a monthly basis after transplantation, mice were bled and the peripheral blood was stained with antibodies against Thy1.1 and haematopoietic markers to confirm reconstitution.

CD45-Cre knock-in mice were bred with R26R to obtain CD45-Cre/R26R mice. The β -gal expression pattern in these mice was examined by X-gal staining of tissues and by fluorescein di- β -D-galactopyranoside (Molecular Probes) staining of haematopoietic cells. Bone marrow cells were incubated for 5 min at 37°C with 10 mM fluorescein di- β -D-galactopyranoside in a hypotonic solution (1:1 staining medium (HBSS plus 2% calf serum): distilled water). Haematopoietic stem cells (Sca-1⁺ c-Kit⁺ Flk-2⁻ lineage⁺ cells)³⁰ were analysed for β -gal expression using a FACS Vantage flow-cytometer (Becton-Dickinson) (Supplementary Fig. 3a).

Tissue collection After 2, 4 or 10 months mice were anaesthetized and transcardially perfused with 0.9% saline followed by 50 ml 4% paraformaldehyde or 2% paraformaldehyde plus 0.25% glutaraldehyde. Brain, spinal cord, liver, lung, kidney, heart, skeletal muscle and gut were dissected. Brain and one liver lobe were serially cut in 50- μm vibratome sections. The rest of the liver and other tissues were cryopreserved and frozen in optimum cutting temperature compound (Sakura-Finectec) at -80°C . Serial 10- or 50- μm sections were cut in a cryostat and stained with X-gal or by immunohistochemistry.

X-gal staining and immunohistochemistry Specimens were placed in phosphate buffer containing 10 mM $\text{K}_3\text{Fe}(\text{CN})_6$ and 10 mM $\text{K}_4\text{Fe}(\text{CN})_6$ along with the β -gal substrate X-gal (1 mg ml^{-1}) (Molecular Probes) at 37°C for 8–12 h. Antibodies against albumin (A-6684; 1:100) and calbindin (C-9848; 1:1,000) were from Sigma, cardiac troponin I (sc-1881; 1:1,000) was from Santa Cruz Biotechnology, BrdU (M0744; 1:100) was from DAKO, CD45 (558750; 1:100) was from BD Pharmingen, and Iba1 was a gift from Y. Imai. Secondary antibodies anti-mouse-, goat- or rabbit-IgG (H + L) (Cy-2, 1:400; Cy-3, 1:400; biotinylated, 1:500) conjugated were from Jackson Immunoresearch.

Plastic embedding and electron microscopy Fifty- μm sections were post-fixed with 1% osmium and 7% glucose for 2 h, rinsed, dehydrated and embedded in araldite (Durcupan, Fluka). Semi-thin sections (1.5 μm) were cut with a diamond knife and stained lightly with 1% toluidine blue. Semi-thin sections were re-embedded in an araldite block and detached from the glass slide by repeated freezing (liquid nitrogen) and thawing. Ultra-thin (0.05 μm) sections were cut with a diamond knife, stained with lead citrate and examined under a Jeol 100CX electron microscope.

Supplementary information accompanies this paper.

Received 18 August 2003; accepted 24 September 2003

http://www.nature.com/cgi-taf/DynaPage.taf?file=/nature/journal/v425/n6961/full/nature02069_r.html&filetype=&dynoptions=

1/10/04

References

1. Morrison, S. J. Stem cell potential: can anything make anything? *Curr. Biol.* **11**, R7-R9 (2001) | [Article](#) | [PubMed](#) | [ISI](#) | [ChemPort](#) | (2002) | [Article](#) | [PubMed](#) | [ISI](#) | [ChemPort](#) |
2. Orkin, S. H. & Zon, L. I. Hematopoiesis and stem cells: plasticity versus developmental heterogeneity. *Nature Immunol.* **3**, 323-328 (2002) | [Article](#) | [PubMed](#) | [ISI](#) | [ChemPort](#) |
3. Krause, D. S. *et al.* Multi-organ, multi-lineage engraftment by a single bone marrow-derived stem cell. *Cell* **105**, 369-377 (2001) | [PubMed](#) | [ISI](#) | [ChemPort](#) |
4. Orlic, D. *et al.* Bone marrow cells regenerate infarcted myocardium. *Nature* **410**, 701-705 (2001) | [Article](#) | [PubMed](#) | [ISI](#) | [ChemPort](#) | (2001) | [Article](#) | [PubMed](#) | [ISI](#) | [ChemPort](#) |
5. Priller, J. *et al.* Neogenesis of cerebellar Purkinje neurons from gene-marked bone marrow cells *in vivo*. *J. Cell Biol.* **155**, 733-738 (2002) | [Article](#) | [PubMed](#) | [ISI](#) | [ChemPort](#) |
6. Terada, N. *et al.* Bone marrow cells adopt the phenotype of other cells by spontaneous cell fusion. *Nature* **416**, 542-545 (2002) | [Article](#) | [PubMed](#) | [ISI](#) | [ChemPort](#) |
7. Ying, Q. L., Nichols, J., Evans, E. P. & Smith, A. G. Changing potency by spontaneous fusion. *Nature* **416**, 545-548 (2002) | [Article](#) | [PubMed](#) | [ISI](#) | [ChemPort](#) |
8. Vassilopoulos, G., Wang, P. R. & Russell, D. W. Transplanted bone marrow regenerates liver by cell fusion. *Nature* **422**, 901-904 (2003) | [Article](#) | [PubMed](#) | [ISI](#) | [ChemPort](#) |
9. Wang, X. *et al.* Cell fusion is the principal source of bone-marrow-derived hepatocytes. *Nature* **422**, 897-901 (2003) | [Article](#) | [PubMed](#) | [ISI](#) | [ChemPort](#) |
10. Sauer, B. Inducible gene targeting in mice using the Cre/lox system. *Methods* **14**, 381-392 (1998) | [Article](#) | [PubMed](#) | [ISI](#) | [ChemPort](#) |
11. Lewandoski, M., Meyers, E. N. & Martin, G. R. Analysis of Fgf8 gene function in vertebrate development. *Cold Spring Harb. Symp. Quant. Biol.* **62**, 159-168 (1997) | [PubMed](#) | [ISI](#) | [ChemPort](#) |
12. Mao, X., Fujiwara, Y. & Orkin, S. H. Improved reporter strain for monitoring Cre recombinase-mediated DNA excisions in mice. *Proc. Natl Acad. Sci. USA* **96**, 5037-5042 (1999) | [Article](#) | [PubMed](#) | [ChemPort](#) |
13. Janus, A., Holz, G. G., Theise, N. D. & Hussain, M. A. *In vivo* derivation of glucose-competent pancreatic endocrine cells from bone marrow without evidence of cell fusion. *J. Clin. Invest.* **111**, 843-850 (2003) | [Article](#) | [PubMed](#) | [ISI](#) | [ChemPort](#) |
14. Weiss, S. *et al.* Multipotent CNS stem cells are present in the adult mammalian spinal cord and ventricular neuroaxis. *J. Neurosci.* **16**, 7599-7609 (1996) | [PubMed](#) | [ISI](#) | [ChemPort](#) |
15. Palay, L. P. & Chan-Palay, V. *Cerebellar Cortex* 15-25 (Springer, Berlin, 1974)
16. Weimann, J. M., Charlton, C. A., Brazelton, T. R., Hackman, R. C. & Blau, H. M. Contribution of transplanted bone marrow cells to Purkinje neurons in human adult brains. *Proc. Natl Acad. Sci. USA* **100**, 2088-2093 (2003) | [Article](#) | [PubMed](#) | [ChemPort](#) |
17. Wagers, A. J., Sherwood, R. I., Christensen, J. L. & Weissman, I. L. Little evidence for developmental plasticity of adult hematopoietic stem cells. *Science* **297**, 2256-2259 (2002) | [Article](#) | [PubMed](#) | [ISI](#) | [ChemPort](#) |
18. Ledbetter, J. A. & Herzenberg, L. A. Xenogeneic monoclonal antibodies to mouse lymphoid differentiation antigens. *Immunol. Rev.* **47**, 63-90 (1979) | [PubMed](#) | [ISI](#) | [ChemPort](#) |
19. van Ewijk, W., van Soest, P. L. & van den Engh, G. J. Fluorescence analysis and anatomic distribution of mouse T lymphocyte subsets defined by monoclonal antibodies to the antigens Thy-1, Lyt-1, Lyt-2, and T-200. *J. Immunol.* **127**, 2594-2604 (1981) | [PubMed](#) | [ChemPort](#) |
20. Ling, E. A. & Wong, W. C. The origin and nature of ramified and amoeboid microglia: a historical review and current concepts. *Glia* **7**, 9-18

(1993) | [PubMed](#) | [ISI](#) | [ChemPort](#) |

21. Gehrmann, J., Matsumoto, Y. & Kreutzberg, G. W. Microglia: intrinsic immunoeffector cell of the brain. *Brain Res. Brain Res. Rev.* **20**, 269-287 (1995) | [Article](#) | [PubMed](#) | [ChemPort](#) |
22. Arias, I. M., et al. *The Liver Biology and Pathobiology* (Lippincott Williams and Wilkins, Philadelphia, 2001)
23. Anderson, J. M. Multinucleated giant cells. *Curr. Opin. Hematol.* **7**, 40-47 (2000) | [Article](#) | [PubMed](#) | [ISI](#) | [ChemPort](#) |
24. Piper, H. M. & Isenberg, I. *Isolated Adult Cardiomyocytes* (CRC, Boca Raton, 1989)
25. Lapham, L. W. Tetraploid DNA content of Purkinje neurons of human cerebellar cortex. *Science* **159**, 310-312 (1968) | [PubMed](#) | [ISI](#) | [ChemPort](#) |
26. Mares, V., Lodin, Z. & Sacha, J. A cytochemical and autoradiographic study of nuclear DNA in mouse Purkinje cells. *Brain Res.* **53**, 273-289 (1973) | [Article](#) | [PubMed](#) | [ISI](#) | [ChemPort](#) |
27. Doetsch, F., Caille, I., Lim, D. A., Garcia-Verdugo, J. M. & Alvarez-Buylla, A. Subventricular zone astrocytes are neural stem cells in the adult mammalian brain. *Cell* **97**, 703-716 (1999) | [PubMed](#) | [ISI](#) | [ChemPort](#) |
28. Spector, D. L., Goldman, R. D. & Leinwand, L. A. *Cells: a Laboratory Manual* 4.1-4.7 (Cold Spring Harbor Laboratory Press, New York, 1998)
29. Hadjantonakis, A. K., Gertsenstein, M., Ikawa, M., Okabe, M. & Nagy, A. Generating green fluorescent mice by germline transmission of green fluorescent ES cells. *Mech. Dev.* **76**, 79-90 (1998) | [Article](#) | [PubMed](#) | [ISI](#) | [ChemPort](#) |
30. Christensen, J. L. & Weissman, I. L. Flk-2 is a marker in hematopoietic stem cell differentiation: a simple method to isolate long-term stem cells. *Proc. Natl Acad. Sci. USA* **98**, 14541-14546 (2001) | [Article](#) | [PubMed](#) | [ChemPort](#) |

Acknowledgements. The authors thank G. Martin and P. Soriano for transgenic mouse lines, J. Maher at the UCSF Liver Centre for advice and assistance, and M. Kiel, O. Yilmaz and The University of Michigan Flow Cytometry Core for help with flow cytometry. R.P. thanks E. Schaller for technical help. M.A-D. thanks B. Rico, I. Cobos, T. Aragon and U. Borello for personal and scientific support. This work was supported by grants from NIH, the Sandler Foundation, the Spanish Ministry of Science and Technology (Ataxias Cerebelosa), and the Deutsche Forschungsgemeinschaft (DFG). R.P. was the recipient of a postdoctoral fellowship from the Spanish Ministry of Science and Technology.

Competing interests statement. The authors declare that they have no competing financial interests.